Journal of Catalysis **194,** 352–363 (2000)
doi:10.1006/jcat.2000.2947, available online at http://www.idealibrary.com on IDEAL®

Methyl Side Chain Formation on the $CrCp_2/SiO_2$ Catalyst during Polymerisation of Ethylene: Spectroscopic Analyses and Theoretical Modelling

Richard Blom,[1] Ivar M. Dahl, and Ole Swang

SINTEF Applied Chemistry, P.O. Box 124, N-0314 Oslo, Norway

Received February 7, 2000; revised May 9, 2000; accepted May 24, 2000

Polymerisations at different ethylene pressures and temperatures in the presence of deuterium as a chain transfer agent have been performed with a $CrCp_2/SiO_2$ catalyst. The polymers formed have been analysed by ^1H, ^2H, and ^{13}C NMR spectroscopy. The results from the NMR analyses, DRIFTS analysis of the catalyst in the presence of ethylene, and theoretical modelling (DFT) have been used to investigate the mechanism for methyl branch formation. Indirect evidence for the presence of an isomerised chromium site has been found, where the chromium is bonded to a secondary carbon atom within the polymer chain. The DFT calculations indicate an energy barrier of 17 kcal/mol for the isomerisation, where a hydrogen atom is transferred from the α-carbon to the β-carbon through an olefin–chromium–hydrid intermediate. Propagation from the isomerised site gives a methyl branch. Ethyl branches are also observed, which may be explained by repeated isomerisation. The energy barrier for propagation from the isomerised site is significantly higher than for the regular site where chromium is bonded to the chain end, with barriers of 12 and 8 kcal/mol, respectively. The results support a model in which the observed strong pressure dependence of the activity on the partial pressure of ethylene is due to a higher rate of isomerisation than propagation from this site at low ethylene pressures.

1. INTRODUCTION

The Union Carbide catalyst, which is synthesised by reaction of $CrCp_2$ with calcined silica, is a very active catalyst for polymerisation of ethylene (1). Karol and co-workers have studied the kinetics of the catalyst when polymerising ethylene alone and in the presence of hydrogen as a chain transfer agent (2). Also, the formation of methyl side branches was studied in an indirect way by relating the number of branches to the density of the polymer (3). The ability to produce methyl side branches is uncommon among ethylene polymerisation catalysts, as no methyl branches can be observed for other heterogeneous chromium-based catalysts (CrO/SiO_2 or Silylchromate/SiO_2) or for Ziegler catalysts when homo-polymerising ethylene. For the CrO/SiO_2 catalyst branches with even numbers of carbon atoms are observed if metal alkyls are used (4). Such branches are most probably formed by incorporation of 1-olefins formed *in situ* on oligomerising sites that have been induced by the metal alkyls. Methyl side chains must be formed by another mechanism. For cationic nickel–diimine complexes, a significant amount of methyl branches, and longer branches as well, are observed in oligomerisation and polymerisation of ethene (5). A chain isomerisation mechanism is proposed in which a terminally bonded polymer (or oligomer) chain is transferred into a secondary bonded chain via β-hydride elimination and reinsertion. An intermediate is the nickel hydride-olefin species. Theoretical modelling of the chain isomerisation steps show that the energy barriers for this, following the proposed mechanism, are within reasonable values (6).

We have recently studied the formation of methyl side chains as a function of the ethylene pressure when polymerising with the $CrCp_2/SiO_2$ catalyst (7). The number of methyl branches, as well as transvinylene and vinyl fragments, were measured by spectroscopic methods, thus allowing quantitative kinetic relations to be estimated. A kinetic scheme for the different propagation, termination, and isomerisation steps was then developed based on the reaction scheme of Karol *et al.* (2). This is shown in Scheme 1.

In the kinetic analyses, we found that a model in which the equilibrium between the regular polymerisation sites, Cr_o, and the isomerised sites, Cr_i, is shifted towards the isomerised site at low ethylene pressures fit well to the experimental data. This reduction in the number of regular sites can explain the strong pressure dependence on the polymerisation activity observed for this catalyst if one assumes that propagation from an isomerised site is much slower than propagation from a regular site. In the present paper, DRIFTS analyses have been carried out to get more information about the temperature effects on the methyl side chain formation. In order to verify the existence of the isomerised sites further, ethylene polymerisations at different pressures in the presence of deuterium as a chain

[1] To whom correspondence should be addressed. E-mail: richard.blom@chem.sintef.no.

0021-9517/00 $35.00

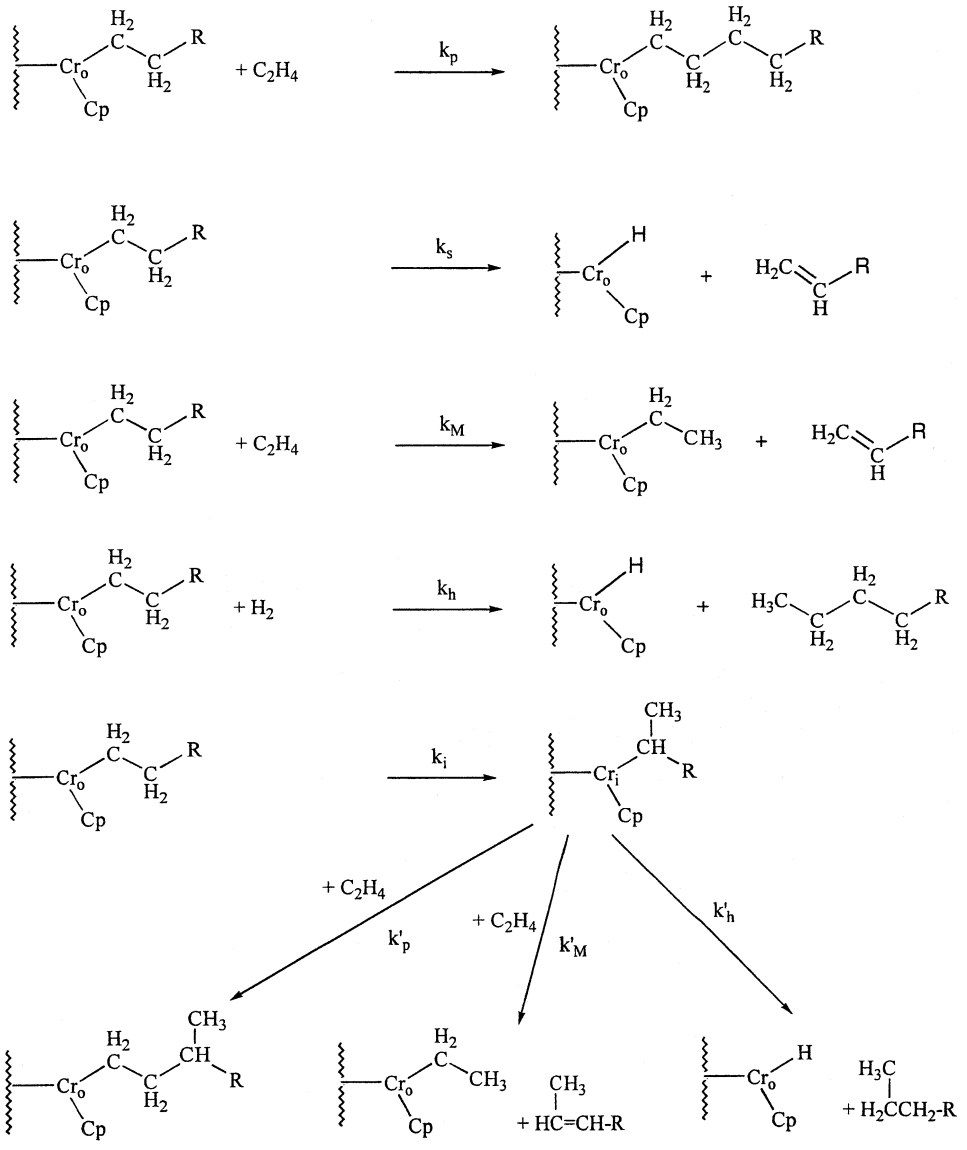

SCHEME 1

termination agent have been performed. In addition, quantum chemical calculations (DFT) of the isomerisation reaction, as well as the first propagation step from both the regular and isomerised site, have been carried out on model systems.

2. METHODS

All handling of catalysts and catalyst precursors were carried out under argon atmosphere (>99.9999%) either by using Schlenck techniques or in a glove box. All solvents used were purified by standard techniques.

Catalyst Preparation

The $CrCp_2/SiO_2$ catalyst, containing 1.0 wt% Cr, was prepared in the following manner: 5.1 g silica, which had been calcined in dry air at 800°C for 16 h, was added to a round neck bottle containing a filter unit in a glove box. The bottle was closed and transferred to a vacuum line. Fifty mililiters of pentane was added by using a syringe to make a slurry. Two hundred nine miligrams of $CrCp_2$ was added to a separate Thomas bottle. Ten mililiters of toluene was then added to the Thomas bottle to make a $CrCp_2$/toluene solution. $CrCp_2$/toluene solution (8.54 ml) was slowly added to the silica/pentane suspension under continuos stirring by using a syringe. After all $CrCp_2$/toluene had been added (10 min), the slurry was stirred for another 30 min. The slurry was then filtrated, and the solid rest was dried under reduced pressure for about 1 h to yield a free-flowing dry blackish powder. The round neck bottle was then transferred to the glove box for storage.

Ethylene Polymerisation

Ethylene polymerisation experiments in the presence of deuterium as a chain termination agent was carried out in a reactor rig described in (8). Deuterium was added at the beginning of the experiment. Some polymerisations, at low partial pressures of ethylene, were performed in the gas phase in sealed 36-ml Thomas bottles containing a magnetic stirrer. One gram of catalyst was used in each run. Ethylene was added on demand through a syringe to keep a constant pressure, while deuterium was added by a separate 5-ml gas-tight Hamilton syringe to ensure the presence of deuterium during the polymerisation. The ambient temperature polymerisation was carried out without any external cooling, while the experiments at 90°C were carried out by placing the Thomas bottle in an oil bath kept at the desired temperature.

DRIFTS Analyses

Diffuse reflectance infrared Fourier transform spectroscopic (DRIFTS) analyses were carried out in a manner similar to that described by Bade *et al.* (9). Ethylene was added at a constant flow into a constant argon flow through the DRIFTS cell. Typically, an argon flow of 50 ml/min was used and the ethylene flow was varied between 0.9 and 5.0 ml/min. For the spectra shown in Fig. 1, the spectra of the catalyst prior to ethylene exposure have been used as backgrounds.

NMR Analyses

^{1}H, ^{2}H, and ^{13}C NMR analyses of polyethylene samples were carried out on a Varian VXR 300S instrument. For polymers produced at low productivities (g_{PE}/g_{cat}) at atmospheric ethylene pressure the polymer was separated from the catalyst remains (mainly silica) by dissolution in 40% HF solution (p.a. from Merck). After removal of the HF solution, the solid rest was washed once with HF solution and three times with distilled water before drying the polymer at 80°C overnight. For NMR analyses, a certain mass of the polymer was added together with 0.5 ml of either 1,2-dichlorobenzene (^{2}H NMR) or d_4-1,2-dichlorobenzene (^{1}H and ^{13}C NMR) to a 5-mm NMR tube. The tube was then evacuated and sealed before dissolution of the polymer was carried out at 130°C. In the ^{2}H NMR spectra, the natural abundance of deuterium in 1,2-dichlorobenzene was used as internal standard, where the peak stemming from the deuterium in 4 position (the right peak) was set to δ7.00 ppm. For the ^{1}H NMR analyses, the small amount of undeuterated solvent was used as an internal standard; the hydrogen in 4 position (the right peak) was set to δ7.00 ppm. For the ^{13}C NMR analyses the main peak from the polymer chain was used as an internal standard and was set to δ29.98 ppm. In order to obtain quantitative data in the ^{13}C NMR experiments, a delay time of 60 s was used.

Computational Details

The DFT calculations were carried out using the program system ADF developed by Baerends *et al.* (10). The frozen-core approximation was used for all atoms except hydrogen, keeping the orbitals up to and including 2*p* for Cr and Si, and 1*s* for O and C frozen in their atomic shapes. The orbitals were described by Slater-type orbital (STO) basis sets. The number of unfrozen basis functions, in order of increasing angular momentum, is (5, 3, 3) for chromium, (3, 3, 1) for oxygen, (2, 2, 1) for silicon and carbon, and (2, 1) for hydrogen, yielding TZVP quality for Cr and O and DZVP for the other atoms (note that the number of unfrozen orbitals is larger than the number of valence orbitals). Slater exchange and the VWN parameterisation of the LDA correlation energy (11), with the gradient corrections of Becke (12) for exchange and of Perdew (13) for correlation, were used for the exchange-correlation energies; the gradient corrections were added self consistently. The accuracy of the numerical integration was set to $10^{-5.0}$, which may be assumed to give a numerical noise level of less than 0.1 kcal/mole in the final energies (14). In some cases, an accuracy of $10^{-6.0}$ was necessary to achieve geometry convergence. The calculations were carried out making no assumptions of molecular symmetry. The systems under study have an uneven number of electrons. Several of the stationary points were optimised with both doublet and quartet multiplicity, and quartet electronic states proved the most stable in all cases. Hence, all results reported here are for species of quartet multiplicity. The calculations were run unrestrictedly, with separate sets of Kohn–Sham orbitals for each spin. For reasons of computational economy, no vibrational spectra were calculated. The silica surface has been modelled by a single $Si(OH)_3(O)^-$ unit (see Fig. 5), and the results do not include zero-point energy corrections or any description of entropy. With this in mind, the absolute reaction and activation energies must be regarded as semi-quantitative only. However, quantum chemical cluster modelling of surface reactions has proven to be a useful tool for the description of energy trends for more than a decade (15). The transition states were found by stepping the chosen reaction coordinate, thereby allowing all other geometrical degrees of freedom to relax. Exceptions here are the ethylene insertion transition states, which were optimised explicitly.

3. RESULTS

Ethylene Polymerisation

Ethylene polymerisations were carried out at different partial pressures of ethylene with deuterium as a chain transfer agent. The conditions used in the different polymerisations as well as the obtained polymer yields are given in Table 1. The activities at low ethylene pressures are low,

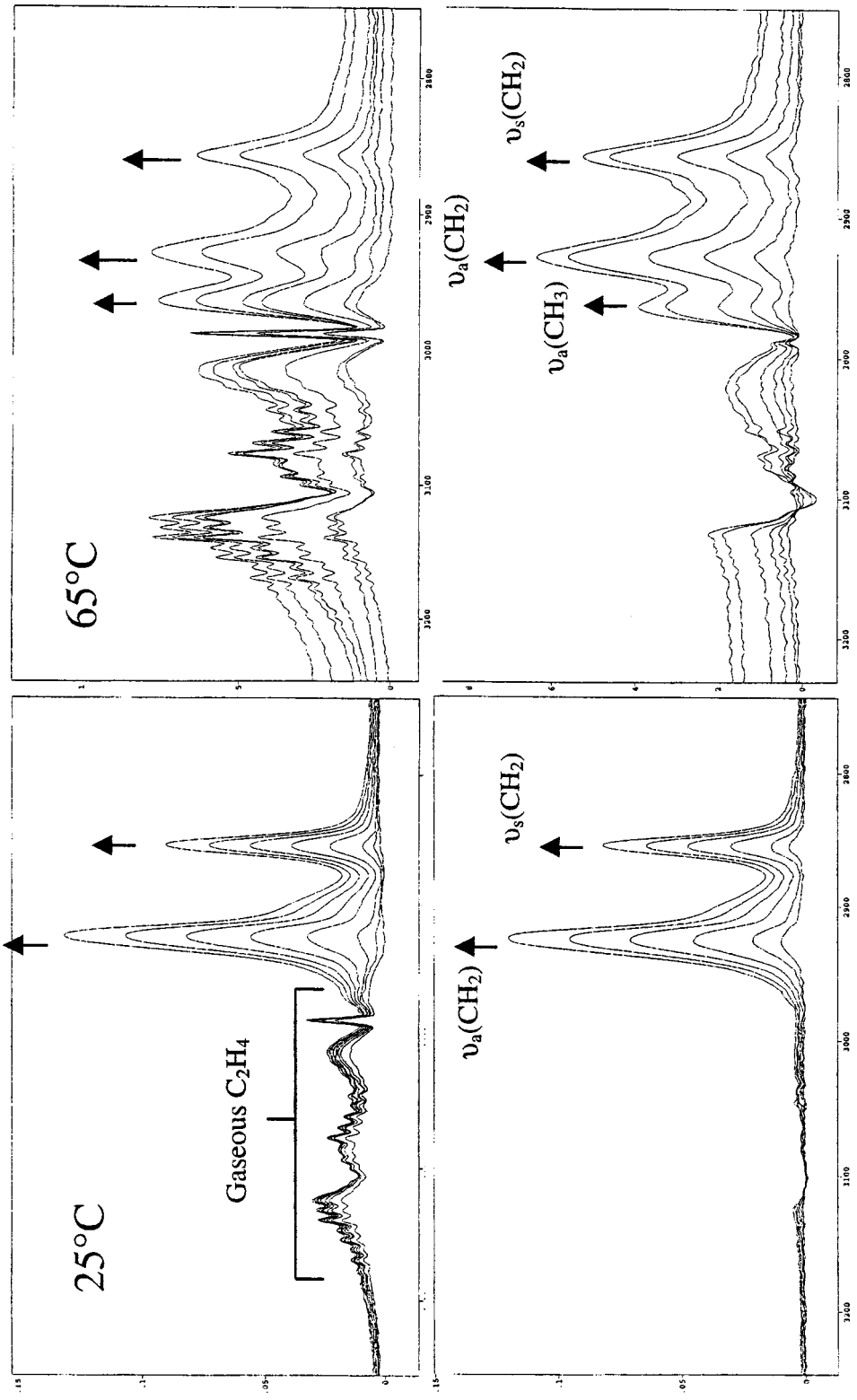

FIG. 1. DRIFT spectra recorded under ethylene flow at different times on stream for the C–Hstretch region. (top) Raw spectra at 25 and 65°C with spectrum in the absence of ethylene used as background; (bottom) spectra obtained when using one of the first spectra in the presence of ethylene as background.

TABLE 1

Details about the Ethylene Polymerisations Carried out in the Presence of Deuterium

Run	p_{total} (atm)	$p(C_2H_4)$ (atm)	$p(D_2)$ (atm)	Temp. (°C)	m_{cat} (g)	polym. time (min)	polym. yield (g)	Activity (g/g/h)
1[a]	39.0	13.8	2.0	90	0.385	60	51.7	134
2[a]	28.5	17.7	2.0	30	0.401	60	31.8	79
3[a]	20.5	1.1	1.0	90	0.490	156	2.8	2.2
4[a]	10.5	3.8	1.0	30	0.556	125	5.3	4.6
5[b]	1.2	1.0	0.2	90	1.00	50	1.2	1.4
6[b]	1.2	1.0	0.2	30	1.00	30	1.0	2.0

[a] Polymerisations carried out in 1 l autoclave using 0.5 l isobutane as a diluent. The total pressure is measured, while the partial pressure of ethylene has been estimated using the Peng–Robinson equation of state. Deuterium is added to the reactor before isobutane, and the pressures noted refer to the partial pressure in the absence of isobutane and ethylene.

[b] Low pressure gas phase polymerisations carried out in Thomas bottles as described in Methods.

as expected, while the activity does not seem to be greatly affected by the temperature.

DRIFTS Analyses

The ν(C–H) region of the DRIFT spectra obtained with $CrCp_2/SiO_2$ at 25 and 65°C when exposed to a constant flow of ethylene/argon are shown in Figs. 1a and 1b, respectively. The spectra have been recorded at different times on stream. At 25°C, only two peaks at 2859 and 2930 cm^{-1} are observed, consistent with ν_s(C–H) and ν_a(C–H) of methylene groups. At 65°C, an additional peak at 2962 cm^{-1} is observed, which is typical for ν_a(C–H) of methyl groups. The ν_s(C–H) mode of methyl groups, usually observed around 2890 cm^{-1} can be observed as a shoulder. The negative peaks observed in the region 3000 to 3100 cm^{-1} is due to the loss of toluene during the experiments. The toluene was introduced in the catalyst preparation as explained in the Methods section.

NMR Analyses

The polymers were analysed by NMR since this method may give direct quantitative information. ^{1}H NMR spectroscopy gives good information about the type of unsaturated species present and the concentration of these in the polyethylene. Vinyl, transvinylene, and vinylidene fragments are the most common. ^{13}C NMR gives quantitative information on the number of methyl end groups, methyl side branches, and also other short chain branches if present. ^{2}H NMR gives information about the relative ratio of deuterated species in the polymer. In our case, deuterated methylene, –CHD–, and deuterated methyl, $–CH_2D$, are the two expected species. We will not show all the spectra recorded, but give typical examples and the numerical values obtained from the quantitative analyses. Figure 2 gives the ^{1}H-NMR spectra of the polymer obtained in runs 1 and 3, respectively. The two polymers have been prepared at 90°C at different partial pressures of ethylene.

The main peak at δ1.4 is from methylene groups, while the peak at δ0.9 is from methyl groups. The region from δ4.5 to δ6.0 gives direct information about the kind and amount of unsaturated species present. The single broad peak observed at δ5.5 is typical of a transvinylene fragment. In order to find out whether the transvinylene is at the end of a chain or is internal we used the two model compounds trans-2-nonene (T2N) and trans-5- decene (T5D). T2N has a transvinylene group in the 2-position, similar to the end group formed after either termination by spontaneous

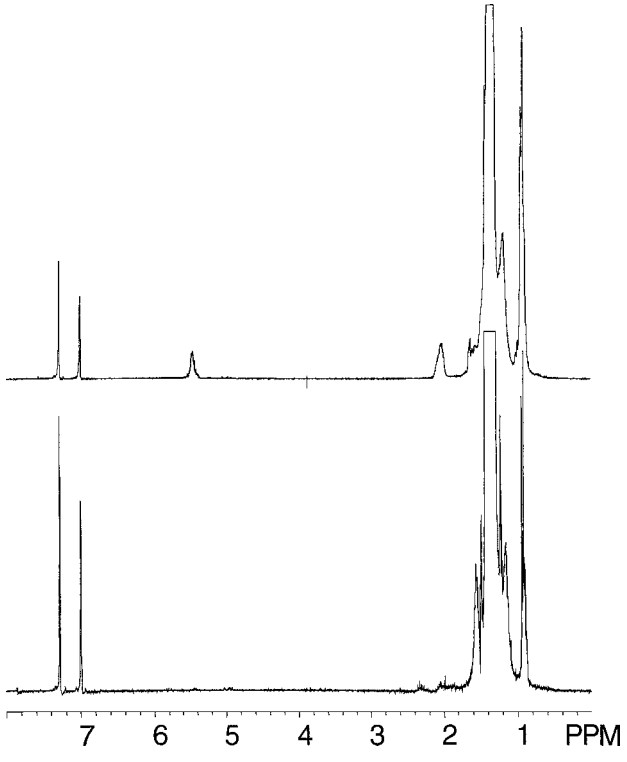

FIG. 2. ^{1}H-NMR spectra of the polymers produced in (bottom) Run 1 and (top) Run 3.

β-hydride elimination or by chain transfer to monomer from a Cr_i site as shown in Scheme 1. On the other hand, T5D will be a model of a transvinylene group farther away from the chain end. The main difference in the ^{1}H NMR spectra of two compounds are (i) the ratio of the areas of the peak of the hydrogen atoms bonded to the sp^2 hybridised carbons (at δ5.5 ppm) relative to that of the hydrogen atoms of the methylene group(s) next to the double bond (at δ2.00 ppm) and (ii) T2N has a separate peak at δ1.65 ppm from the methyl group bonded to a sp^2 hybridised carbon. By comparing the ^{1}H NMR spectra of the polymers with those of the model compounds information about the position of the transvinylene group can be obtained. The polymer prepared at high pressure of ethylene (Run 1) shows negligible amounts of transvinylene, while the polymer prepared at low pressure (Run 3) shows strong peaks at around δ5.5 and δ2.0 together with a shoulder at around δ1.6 (this peak being disturbed by rotational bands of the major $-CH_2-$ peak). The ratio between the peak at δ2.0 and δ5.5 is 1.78, indicating that only about 22% of the double bonds are at the chain end as depicted in Scheme 1, the rest being farther away from the chain end.

Figure 3 shows the ^{13}C NMR spectrum of the same polymers. Following the assignments by Hansen *et al.* (16), the triplet around δ13.7 can be assigned to $-CH_2D$ chain ends with $J^1_{CD} = 72$ Hz A separate peak at δ14.0 stems from undeuterated methyl chain ends, or from branches longer than C_6. The carbons of the methyl side branches give rise to the peak at δ20.0. Interestingly, small peaks are also observed for polymer 3 at δ11.3, δ26.8, δ34.1, and δ39.7 which are specific for ethyl side branches. These peaks were even more pronounced in the spectrum of the polymer from Run 5.

Figure 4 shows the ^{2}H NMR spectra of all six polymers. Two peaks are observed in the spectra, one from –CHD– groups at around δ1.3 and one from $-CH_2D$ groups at around δ0.8. The qualities of the spectra were different due to the different molecular weights of the polymers produced at different temperatures and pressures giving different solubility in 1,2-dichlorobenzene.

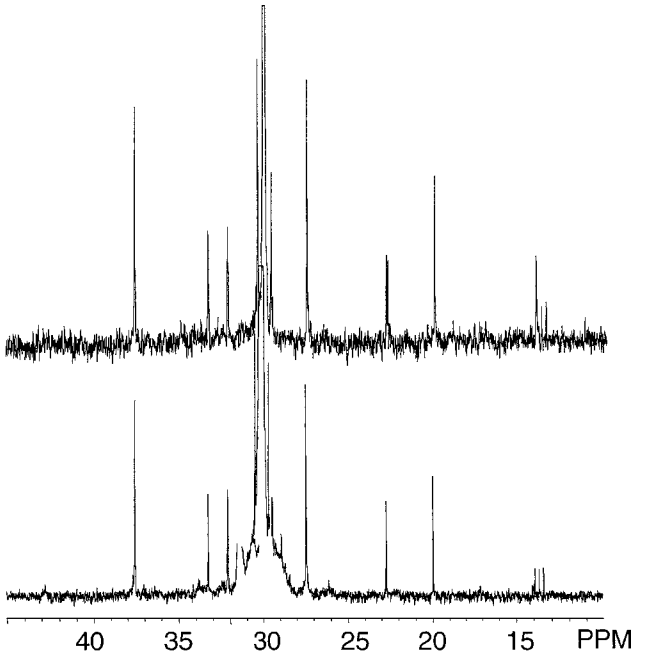

FIG. 3. ^{13}C-NMR spectra of the polymers produced in (bottom) Run 1 and (top) Run 3.

The concentration of the different fragments obtained from the NMR spectra are given in Table 2. Errors in the numbers have been estimated from the signal to noise level of the different spectra. The results can be summarised as follows: A negligible amount of methyl branching is observed when the polymerisation is carried out at

TABLE 2

Results from Fragment Analyses of the Polymers

Run	Me^a_b/1000C ^{13}C-NMR	Et^b_b/1000C ^{13}C-NMR	$(-CH_3)^c_{ce}$/1000C ^{13}C-NMR	$(-CH_2D)^d_{ce}$/1000C ^{13}C-NMR	—/1000C ^{1}H-NMR	$\frac{[-CH_2D]}{[-CHD-]}$ ^{2}H-NMR	$\frac{[Cr_o]}{[Cr_i]}$ Eq. [1]
1	2.0(±0.2)	bdl	0.4(±0.2)	1.1(±0.2)	bdl	6.1(±0.4)	2.6
2	bdl	bdl	bdl	0.5(±0.2)	bdl	4.3(±1.2)	1.7
3	19.4(±0.8)	2.3(±0.9)	8(±1)	6.7(±1.0)	2.8(±0.3)	2.2(±0.2)	0.6
4	bdl	bdl	bdl	2.0(±0.5)	0.2(±0.1)	2.8(±0.8)	0.9
5	20(±2)	1.8(±0.2)	5.1(±0.3)	bdl	2.6(±0.4)	0.5(±0.2)	—
6	—[e]	—[e]	—[e]	—[e]	bdl	1.0(±0.4)	0

Note. The numbers are based on ^{1}H-, ^{2}H-, and ^{13}C-NMR data as indicated. Estimated errors are given in parentheses. bdl = below detection limit.

[a] Methyl side branches.

[b] Ethyl side branches.

[c] Methyl chain ends.

[d] Deuterated methyl chain ends.

[e] The ^{13}C-NMR spectrum obtained was of poor quality and could therefore not be used for quantitative analyses.

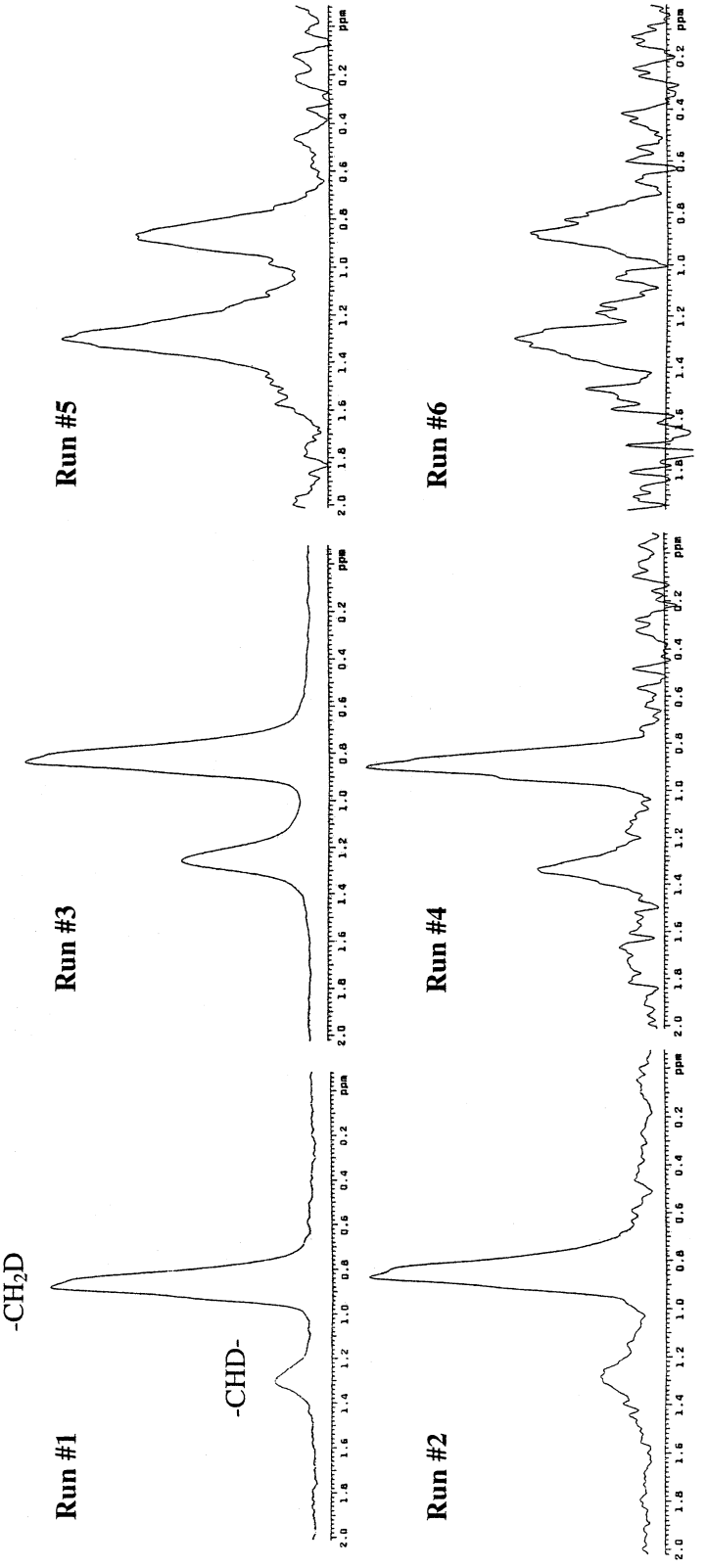

FIG. 4. ^{2}H-NMR spectra of the polymers produced at different temperatures and pressures given in Table 1.

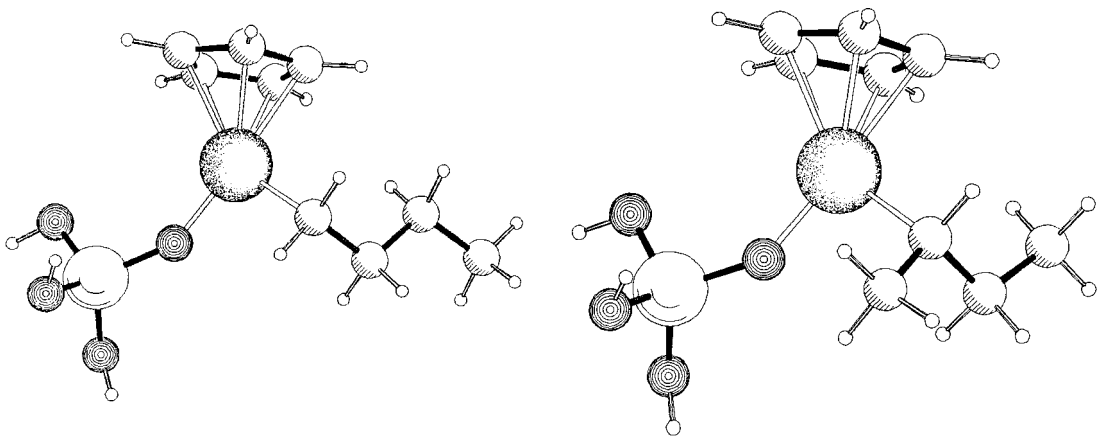

FIG. 5. The molecular model used throughout the theoretical calculations: (left) the regular chromium site, Cr_o; (right) the isomerised chromium site, Cr_i.

low temperatures. At 90°C, a significant amount of methyl branches are observed. Lower partial pressure of ethylene give more methyl branching and also some ethyl branches, which has not been previously observed for this catalyst. Lower ethylene pressure also gives a strong increase in the number of nondeuterated methyl chain ends. Transvinylene fragments are produced more efficiently at low ethylene pressures and elevated temperatures. The $[-CH_2D]/[-CHD-]$ ratio shows a steady decrease with decreased partial pressure of ethylene.

DFT Modelling

Three reactions have been modelled: The isomerisation between the *n*-alkyl and iso-alkyl species and the insertion of ethylene into the Cr–C bond for both species. The molecular model used for the *n*-alkyl and the iso-alkyl sites of the $CrCp_2/SiO_2$ catalyst throughout the theoretical calculations is shown in Fig. 5. Relative energies for different stationary points on the potential energy surfaces (PES) for these reactions can be found in Table 3, and the same energies are plotted in Fig. 6, with nomenclature as defined in Table 3. The β-agostic *n*-butyl site has been taken as the zero energy reference.

The most stable conformer of the *n*-butyl species shows a strong β-agostic interaction. The agostic C–H bond is stretched to 1.17 Å, while the corresponding angle Cr–C_α–C_β is much smaller than tetrahedral at 82°. The calculated stabilisation energy due to the agostic interaction is

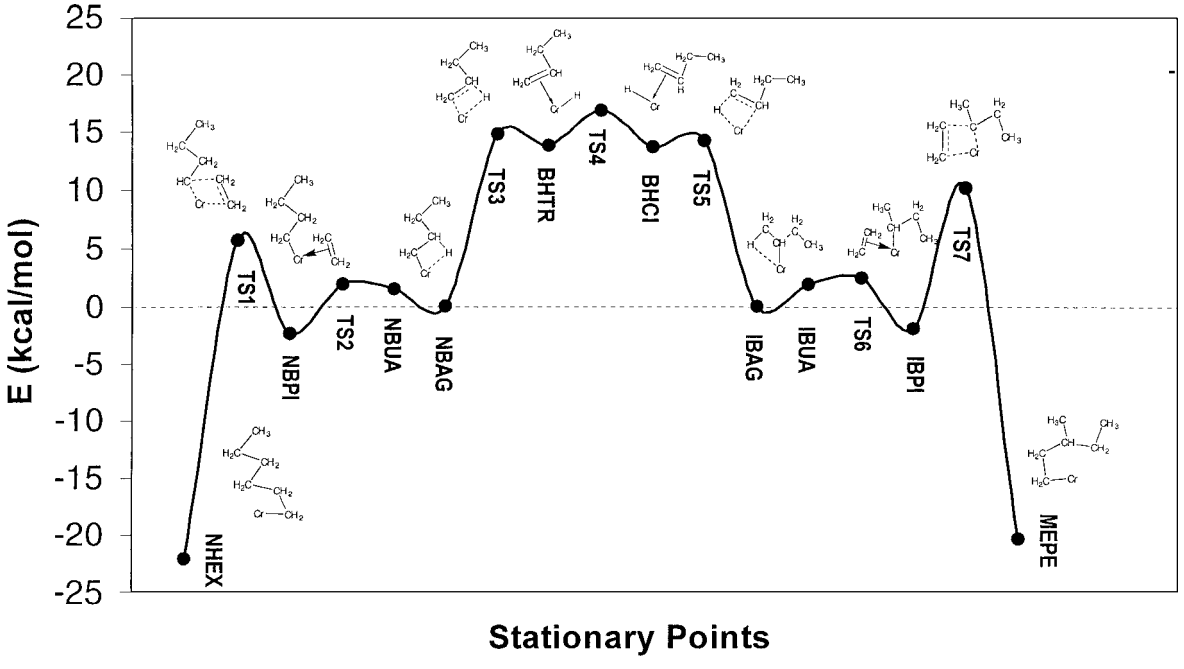

FIG. 6. The energy curve of the (middle) isomerisation reaction and the (left) insertion of ethylene on the regular chromium site and (right) on the isomerised chromium site.

TABLE 3

Relative Energies for Different Species and Abbreviations Used in Fig. 6

Species	Abbreviation (Fig. 6)	E(kcal/mol)
n-hexyl, δ-agostic	NHEX	−22.1
TS	TS1	5.8
n-butyl π-complex	NBPI	−2.3
TS*	TS2	2 (approx.)
n-butyl nonagostic	NBUA	1.6
n-butyl δ-agostic	NBAG	≡0
TS*	TS3	15 (approx.)
π-butene-hydride trans	BHTR	13.8
TS	TS4	17.0
π-butene-hydride cis	BHCI	13.7
TS	TS5	14.3
isobutyl β-agostic	IBAG	0.1
isobutyl nonagostic	IBUA	2.0
TS*	TS6	2.5 (approx.)
isobutyl π-complex	IBPI	−1.9
TS	TS7	10.3
3-methylpentyl δ-agostic	MEPE	−20.3

1.6 kcal/mol. Geometry optimisations were started from α-, γ-, and δ-agostic structures, but they invariably converged to a nonagostic structure. The isobutyl case is quite similar: The agostic C–H bond is stretched to 1.15 Å, while the corresponding angle Cr–C_α–C_β is much smaller than tetrahedral at 81°. The calculated stabilisation energy due to the agostic interaction is 2.0 kcal/mol. Also for this species, geometry optimisations started from α- and γ-agostic structures invariably converged to a nonagostic structure. A doubly β-agostic structure was also attempted, as Thorshaug *et al.* (17) reported such a structure for a cationic zirconocene complex. The optimisation, however, converged to the singly β-agostic structure. We have found no transition state for the conversion between the β-agostic and the nonagostic structures; however, nonagostic structures exist that have small enough energy gradients that the calculations converge under any reasonable convergence criteria. Even if we cannot rigorously prove them to be stationary structures, they are included here for purposes of assessing the strength of the agostic interactions.

The mechanism for isomerisation between *n*-butyl an isobutyl must involve hydrogen transfer from the β to the α carbons, breaking of one metal–carbon bond and forming of another. One could imagine that the hydrogen could stay close both to the metal centre and to the two carbon atoms during the reaction. However, numerous test calculations with the distance between the transferring hydrogen and the α carbon atom as the reaction coordinate showed this reaction to be energetically highly unfavourable. The hydrogen showed no propensity for staying close to the metal.

Another possibility involves C–H bond cleavage leading to an intermediate in which the hydrogen is a regular hydride ligand on the metal, while the butyl chain turns into a 1-buten ligand that is π-bonded to the metal. This reaction path has been described both for a zirconocene-based (17) and for a nickel-diimine-based system (6). Calculations with the distance of the breaking C_β–H bond as reaction coordinate indeed lead to such an intermediate. In order to finish the isomerisation, the butenyl ligand must rotate approximately 180° around an axis roughly through the chromium atom and the midpoint of the C–C double bond. This rotation brings the α-carbon in position for bonding with the hydrogen atom, hence completing the reaction. In Fig. 6, the energy curve for the isomerisation reaction is shown. We note that the transition state between the two stable isomers of the butenylhydride intermediate is the highest point on the curve, giving a barrier of 17 kcal/mole for the isomerisation. Further, the barriers for going from the butenylhydride isomers to the *n*-butyl and iso-butyl structures are both very small.

Turning to the ethylene addition to the two butyl sites, the calculations show that in both cases a preinsertion π complex is formed. During the formation, the agostic interaction is broken. Subsequently, the insertion proceeds through a four-centre transition state, as in the well-known Cossée mechanism, before the insertion product is formed. The energy barrier for insertion into the *n*-butyl and isobutyl structures is 8.1 and 12.2 kcal/mol, respectively, taken as the energy differences between the π complex and the transition state of the insertion. We note that the π complex is more strongly bound for the iso-butyl species, contributing to the higher insertion barrier.

4. DISCUSSION

Our aim with the present study has been to gain a deeper understanding of the mechanisms leading to the formation of methyl side branches on the $CrCp_2/SiO_2$ catalyst. For this, we have applied different spectroscopic methods (DRIFTS and NMR) and quantum chemical modelling. Previous and present results show that a significant number of methyl side branches are formed when polymerising with the $CrCp_2/SiO_2$ catalyst at temperatures around 90°C and low partial pressure of ethylene (7). However, former infrared analyses of the same catalyst carried out at subatmospheric partial pressure of ethylene at ambient temperature show no indication of methyl group formation (18). Actually, the complete lack of peaks corresponding to methyl CH vibration modes have led to the speculation that the active site has a metallacyclic structure (18a). Our first incentive in the present study has therefore been to conduct a careful investigation of the temperature effects on methyl formation for the $CrCp_2/SiO_2$ catalyst.

The DRIFT spectra recorded at 30°C (Fig. 1) is fully consistent with earlier infrared investigations where no peaks

stemming from methyl groups can be observed. However, when the temperature is increased above 60°C, an additional peak around 2960 cm^{-1} is observed, which is typical for the asymmetric stretch of methyl groups. Of course, the DRIFTS analysis cannot tell whether the methyl group is a chain end or a methyl side branch.

The NMR results presented in Table 2 show that a reduction in the partial pressure of ethylene gives a drastic increase in the number of methyl branches. The number of undeuterated methyl chain ends also increases with decreased partial pressure of ethylene. These chain ends are most probably formed by spontaneous β-hydride elimination, which becomes more frequent at low pressures. The methyl peak in the DRIFT spectra is therefore believed to consist of contributions from both the methyl side chains and methyl chain end.

More information on a molecular level about the fragments formed at different temperatures and different pressures has been obtained from a series of ethylene homopolymerisations carried out in the presence of D_2 as chain termination agent. In particular, we are interested in the ratio of deuterated methylene, –CHD–, and deuterated methyl, $–CH_2D$ since this gives indirect information about in which manner chromium is bonded to the polymer chain. From Scheme 1 the following chain termination reactions with deuterium will be expected:

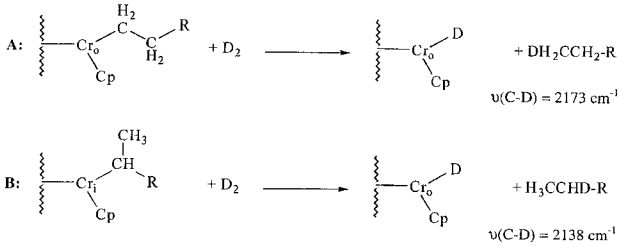

SCHEME 2

The Cr–D species on the right side of the equations will be the start of a new polymer chain giving $–CH_2D$ end groups after ethylene insertion to the Cr–D bond. In sum, reaction **A** of Scheme 2 gives two $–CH_2D$ fragments while reaction **B** gives one –CHD– fragment and one $–CH_2D$ fragment. To a first approximation we can assume no other reactions with deuterium taking place and that the rate constants for chain transfer to hydrogen (deuterium) from Cr_o and Cr_i are equal. The ratio between Cr_i sites and Cr_o sites can then be estimated by using

$$\frac{[Cr_o]}{[Cr_i]} \cong \frac{k_h[Cr_o]}{k'_h[Cr_i]} = \frac{[–CH_2D–]–[–CHD–]}{2[–CHD–]}$$

$$= \frac{[–CH_2D–]}{2[–CHD–]} - 0.5. \qquad [1]$$

Estimates of the ratio between the two kinds of chromium species are given in Table 2. A steady decrease with partial pressure of ethylene is obtained. At 30°C the $[–CH_2D]/[–CHD–]$ ratio reaches a value of 1.0(±0.4) at the lowest partial pressure of ethylene used, corresponding to almost all chromium sites being present as Cr_i sites. At 90°C, a value of the $[–CH_2D]/[–CHD–]$ ratio of 0.5(±0.2) is reached. For the reactions in Scheme 2 the limiting ratio is 1.0, however, isomerisation of a $Cr–CH_2CH_2D$ species followed by propagation will lead to a ratio lower than 1.0. At low ethylene pressure the estimated number of methyl side branches is around 20/1000C. Assuming that the methyl group of an ethyl chain undergoes β-hydride elimination and isomerisation equally rapid as a secondary carbon in a longer alkyl chain, the number of such transformations lead to a theoretical lower limit in the $[–CH_2D]/[–CHD–]$ ratio of 0.92. Such transformation will convert $–CH_2D$ groups into Me_{ce} groups and can then also partly explain the relatively high number of Me_{ce} observed at low ethylene pressures. In the reaction scheme the number of Me_{ce} cannot exceed the sum of unsaturated fragments and the number of –CHD– fragments. For Runs 3 and 5 in Table 2 the number of Me_{ce} falls within this limit.

Additional reactions that convert $–CH_2D$ species into –CHD– species may also occur. We have previously observed –CHD– species when polymerising with a BuLi modified CrO/SiO_2 catalyst at 90°C in the presence of deuterium (4). We then suggested a H/D exchange mechanism at the active site. This mechanism is in principle similar to the one we suggested for the isomerisation reaction, but an additional step must be involved where a Cr–H species is transformed into a Cr–D species by reaction with D_2 under the formation of HD. It may also be that the hydrogen atom in β-agostic interaction with chromium is activated for H/D exchange. It can also be noted that a $[–CH_2D]/[–CHD–]$ ratio lower than 1.0 also can be explained by a metallacyclic structure of the active site (19); however, we cannot see any reasons why an increase in temperature should lead to an increase in the number of metallacyclic sites. We have therefore omitted these speculations in the following discussion.

The DFT calculations indicate that the barrier for the isomerisation reaction is 17 kcal/mol and the barrier for insertion of ethylene into the $Cr_o–C_\alpha$ and $Cr_i–C_\alpha$ bonds are 8 and 12 kcal/mol, respectively. All values are reasonable when considering the simplified model used of the active site throughout the calculations. The lowest energy reaction path of the isomerisation reaction goes through a β-hydride transfer to chromium where the vinyl group formed stays π-coordinated to chromium. Rotation of the double bond followed by reinsertion of the hydrogen on the α-carbon give the isomerised site, Cr_i. A parallel can be drawn to propene polymerisation with ansametallocenes, where a 2,1 insertion of propene leads to a "dormant" site with a high barrier for propagation (20).

The kinetic analyses presented in the previous paper (7) indicated that the rate for propagation from the Cr_i sites is slower than the rate for propagation from the Cr_o sites.

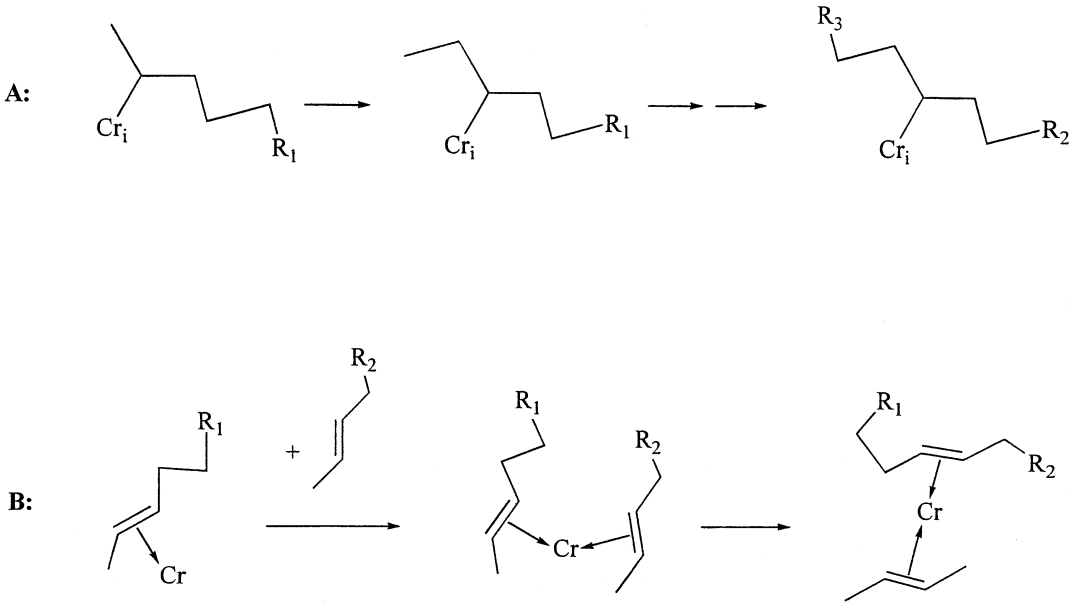

SCHEME 3

The DFT modelling gives a higher barrier for propagation from the Cr_i sites than from the Cr_o sites, which fits well with the kinetic analysis. In the former kinetic analyses the isomerisation was proposed to have a higher rate than propagation form the isomerised site at low partial pressures of ethylene. The DFT calculations give a lower barrier for propagation from the isomerised site than for isomerisation. However, the rate of propagation from the isomerised site will be strongly dependent on the partial pressure of ethylene, which is not the case for the isomerisation. In addition, steric hindrance may reduce the rate of propagation from the isomerised site further. The latter will not be included in the DFT results due to the simplified model used.

Transvinylene can be formed either by chain transfer to ethylene or by spontaneous β-hydride elimination on a Cr_i site (see Scheme 1). In this scheme, such termination leads to a transvinylene with a methyl group on one side. However, the ^{1}H-NMR spectrum given in Fig. 2 indicates that only about 22% of the transvinylene is at the chain end, and that the rest must be situated further from the chain end. This indicates either that transvinylene groups in the polymer are formed not by the route in Scheme 1 or that the 2-transvinylene groups are further transferred into transvinylene groups farther from the chain end, which is energetically more favourable. Such transformations can either occur before the transvinylene group is formed by additional isomerisation reactions at the Cr_i site (by a zipper mechanism) or by metathesis reactions as shown in A and B in Scheme 3.

Path B in the reaction scheme will result in a random distribution of side chains, while path A will give a distribution of side chains with $n(Me_b) > n(Et_b) > n(Pr_b)$, etc. The higher barrier for insertion on the isomerised site from the DFT calculations indicate that propagation from a doubly isomerised site will be even slower, thus leading to a smaller number of longer branches than a Flory distribution would suggest. The ^{13}C-NMR spectrum of the polymers from Runs 3 and 5 give clear evidence for ethyl side branches. No longer branches could be detected, indicating that their number is lower than 0.1–0.2/1000C. Branches with length up to at least C_6 can be selectively observed by ^{13}C NMR, while longer branches will be measured as end groups. Hence, our results support reaction path A.

5. CONCLUSIONS

In agreement with former infrared investigations, we find that DRIFTS analyses of the $CrCp_2/SiO_2$ catalyst in the presence of ethylene show that no detectable amount of methyl groups are formed at ambient temperatures. However, at temperatures above 60°C peaks are observed which can be assigned to methyl groups. The majority of these methyl groups are methyl side branches.

Polymerisations at different partial pressures of ethylene in the presence of deuterium as chain transfer agent, followed by ^{2}H, ^{1}H, and ^{13}C NMR analyses of the polymer formed, give strong evidence for the presence of chromium species, which are not bonded to α-carbons of the growing polymer chains, but rather to secondary carbon atoms in the chains. The number of such isomerised sites, Cr_i, increases with decreased partial pressure of ethylene and with increased polymerisation temperature. Methyl branches, and small amounts of ethyl branches, as well, indicate that the

branches are formed by a zipper mechanism and not by metathesis reactions.

The presence of appreciable amounts of –CHD– at low temperatures, but only small amounts of methyl side branches and transvinylene indicate that we have some isomerisation activity, but that the propagation and termination rates at the isomerised site are low.

DFT modelling of possible isomerisation reaction pathways as well as the propagation step from the regular chromium site, Cr_o, and from the Cr_i site, show that a reasonable isomerisation path can be found for which the energy barrier is calculated to 17 kcal/mol. The propagation from the Cr_i site has a higher barrier than propagation from the Cr_o site, and both propagation steps have lower activation energies than the isomerisation. As $CrCp_2/SiO_2$ does not copolymerise higher 1-olefins, there is obviously strong steric requirements at the active site. The isomerised site will be more sterically demanding than the regular site, thus explaining the lower propagation rate.

ACKNOWLEDGMENTS

We acknowledge generous support from The Research Council of Norway through a Strategic Institute Program (Project No. 110675/420) and the Program for Supercomputing (computer time).

REFERENCES

1. Karol, F. J., Karapinka, G. J., Wu, C., Dow, A. W., Johnson, R. N., and Carrick, W. L., *J. Polym. Sci., Part A-1* **10**, 2621 (1972).
2. Karol, F. J., Brown, G. L., and Davison, J. M., *J. Polym. Sci. Polym. Chem. Ed.* **11**, 413 (1973).
3. Karol, F. J., *in* "Trans. Metal. Catalysed Polym; Ziegler-Natta and Metathesis Polym" (R. P. Quirk, Ed.), p. 702 (1988).
4. Bade, O. M., and Blom, R., *Appl. Catal. A: General* **161**, 249 (1997).
5. Killian, C. M., Tempel, D. J., Johnson, L. K., and Brookhart, M., *J. Am. Chem. Soc.* **118**, 11664 (1996); Svejda, S. A., and Brookhart, M., *Organometallics* **18**, 65 (1999).
6. Musaev, D. G., Froese, R. D. J., Svensson, M., and Morokuma, K., *J. Am. Chem. Soc.* **119**, 367 (1997); Deng, L., Woo, T. K., Cavallo, L., Margl, P. M., and Ziegler, T., *J. Am. Chem. Soc.* **119**, 6177 (1997).
7. Blom, R., Dahl, I. M., Follestad, A., and Jens, K. J., *J. Mol. Catal. A: Chemical* **138**, 97 (1999).
8. Blom, R., and Dahl, I. M., *Macromol. Chem. Phys.* **200**, 442 (1999).
9. Bade, O. M., Blom, R., Dahl, I. M., and Karlsson, A., *J. Catal.* **173**, 460 (1998).
10. Amsterdam Density Functional (ADF), Release 2.3.0, Scientific Computing and Modelling, Dept. of Theoretical Chemistry, Vrije Universiteit, de Boelelaan 1083, 1081 HV Amsterdam. The method is described in the following publications: Baerends, E. J., *Chem. Phys.* **2**, 41 (1973); Baerends, E. J., Ph. D. thesis, Vrije Universiteit Amsterdam, 1975; Ravenek, W., *in* "Algorithms and Applications on Vector and Parallel Computers" (H. J. J. te Riele, T. J. Dekker, and H. A. van de Vorst, Eds.), Elsevier, Amsterdam, 1987; Boerrigter, P. M., te Velde, G., and Baerends, E. J., *Int. J. Quantum Chem.* **33**, 87 (1988).
11. Vosko, S. H., Wilk, L., and Nusair, M., *Can. J. Phys.* **58**, 1200 (1980).
12. Becke, A. D., *Phys. Rev. A* **33**, 2786 (1988); *ACS Symp. Ser.* 394, Washington, DC, 1989; *Int. J. Quantum Chem.* **S23**, 599 (1989); *Phys. Rev. A* **38**, 2398 (1988).
13. Perdew, J. P., *Phys. Rev. B* **33**, 8822 (1986); Erratum in *ibid. B* **34** 7406.
14. te Velde, G., and Baerends, E. J., *J. Comp. Phys.* **99**, 84 (1992).
15. Pacchioni, G., Bagus, P. S., and Parmigiani, F., (Eds.), *in* "Cluster Models for Surface and Bulk Phenomena," NATO ASI Series B Vol. 283, Plenum Press, New York, 1992.
16. Hansen, E. W., Blom, R., and Bade, O. M., *Polymer* **38**, 4295 (1997).
17. Thorshaug, K., Støvneng, J. A., Rytter, E., and Ystenes, M., *Macromolecules* **31**, 7149 (1998).
18. (a) Zecchina, A., Spoto, G., and Bordiga, S., *Faraday Discuss. Chem. Soc.* **87**, 147 (1989); (b) Fu, S.-L., Rosynek, M. P., and Lunsford, J., *Langmuir* **7**, 1179 (1991).
19. First isomerisation of both Cr-C bonds, followed by chain transfer to D_2 on both sides yield two -CHD- species. The di-deutero chromium(IV) species formed can be transformed into the chromium(II) starting point by reductive elimination of D_2. From our results, we cannot exclude this possibility.
20. Busico, V., Cipullo, R., Chadwick, J. C., Modder, J. F., and Sudmeijer, O., *Macromolecules* **27**, 7538 (1994).